The band structure and Fermi surface of $(Sr_3Sc_2O_5)Fe_2As_2$

2009 J. Phys.: Condens. Matter 21 415702

(http://iopscience.iop.org/0953-8984/21/41/415702)

J. Phys.: Condens. Matter **21** (2009) 415702 (5pp) doi:10.1088/0953-8984/21/41/415702

The band structure and Fermi surface of $(Sr_3Sc_2O_5)Fe_2As_2$

Guangtao Wang[1], Yongcheng Liang[2], Lihua Zheng[1] and Zongxian Yang[1]

[1] College of Physics and Information Engineering, Henan Normal University, Xinxiang, Henan 453007, People's Republic of China
[2] College of Engineering Science and Technology, Shanghai Ocean University, Shanghai 200090, People's Republic of China

Received 14 June 2009, in final form 31 August 2009
Published 23 September 2009
Online at stacks.iop.org/JPhysCM/21/415702

Abstract

Inspired by the experience in CuO-based superconductor that a larger spacing distance between CuO planes induced a higher T_C, some researchers synthesized $(Sr_3Sc_2O_5)Fe_2As_2$ and related compounds with spacing distances between FeAs planes as large as 15 Å and expected a higher T_C. Our density functional calculations indicate that the Fermi surface of $(Sr_3Sc_2O_5)Fe_2As_2$ is very similar to that of LaOFeAs, while the projected band structure shows some differences. From Fermi surface nesting and the calculated Lindhard response function $\chi(q)$, we predict that a spin density wave (SDW) and stripe antiferromagnetism (AF) may exist in the undoped compound and that electron or hole doping will suppress this SDW state. Similar to LaFeAsO, both the stabilization energy and the moment are very sensitive to the As atom positions. Because of the considerable similarity to LaFeAsO, $(Sr_3Sc_2O_5)Fe_2As_2$ is expected to become a superconductor with electron or hole doping.

(Some figures in this article are in colour only in the electronic version)

The recent discovery [1] of superconductivity in the FeAs-based compound $LaFeAsO_{1-x}F_x$ with a transition temperature $T_C = 26$ K has generated great excitement. Subsequently, other related compounds $LnFeAsO_{1-x}F_x$ (Ln = Sm, Nd, Ce) have been synthesized with T_C ranging from 10 K to as high as 55 K [2–5]. This series of compounds crystallized in ZrCuSiAs structure and have often been abbreviated as FeAs-1111 systems. Later, three new series of compounds: $A_{1-x}K_xFe_2As_2$ (A = Ba, Sr, Ca and Eu, denoted as FeAs-122) [6–10], Li_xFeAs (FeAs-111) [11–13] and $FeSe_{1-x}$ (FeAs-11) [14], have been reported with their maximum T_C at about 38 K, 18 K and 8 K, respectively.

The common features of the above-mentioned FeAs-based superconductive compounds are that their phases adopt quasi-two-dimensional crystal structures in which superconducting [FeAs] layers are separated by either [LnO] and [AO] layers or Li atomic sheets, which act as a 'charge reservoir'. After analyzing the relationship between the maximum transition temperature T_C and the spacing distance between neighboring FeAs layers (d_{FeAs}), we find an interesting trend that T_C increases with d_{FeAs} increasing (Li_xFeAs: $T_C = 18$ K, $d_{FeAs} = 6.4$ Å; $A_{1-x}K_xFe_2As_2$: $T_C = 38$ K, $d_{FeAs} = 6.5$ Å; SmFeAsOF: $T_C = 55$ K, $d_{FeAs} = 8.7$ Å) [2–8, 12, 13]. Such a trend has also been revealed in Cu-based superconductors. For the single-layer system such as $La_{1-x}Sr_xCuO_4$ and $Bi_2Sr_2CuO_6$ their maximum T_C is about 38 K. With increasing spacing distance between neighboring CuO layers in a double-layer system, such as $YBa_2Cu_3O_7$ and $Bi_2Sr_2CaCu_2O_8$, their maximum T_C increases up to 92 K. For a triple-layer system $Bi_2Sr_2Ca_2Cu_3O_{10}$ its spacing distance further increases, accompanied with T_C increasing to 123 K. Inspired by the experience in CuO-based superconductors, some researchers believed that the larger spacing distance may lead to a higher T_C and they started to look for FeAs-based compounds with larger d_{FeAs}. Indeed, some FeAs-based compounds with d_{FeAs} as large as 15 Å had been fabricated successfully by different groups [15–20] and have been studied by first-principles calculations [21]. Among these compounds, $Sr_4Sc_2Fe_2P_2O_6$ [16] and $Sr_4V_2Fe_2As_2O_6$ [20] became superconductors at about 17 K and 37.2 K, respectively. Comparing with LaOFeP, the maximum T_C of $Sr_4Sc_2Fe_2P_2O_6$ increases from about 4–17 K with d_{FeAs} increasing from 8.5 to 15 Å. Such a relation between maximum T_C and d_{FeAs} makes researchers expect $Sr_4Sc_2Fe_2As_2O_6$ and $(Sr_3Sc_2O_5)Fe_2As_2$ to have a larger T_C than that of

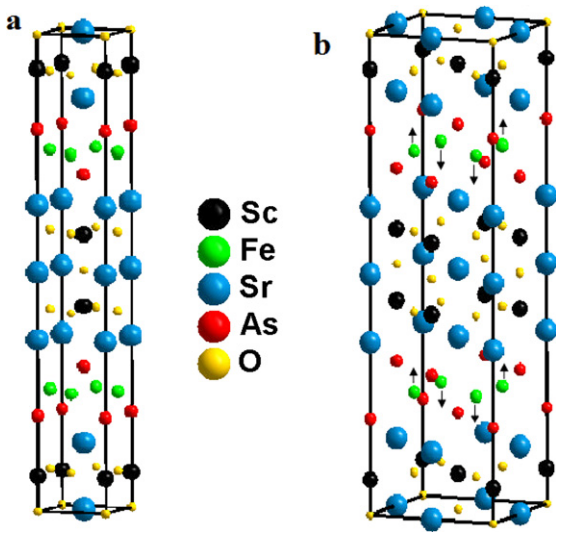

Figure 1. Crystal structures of $(Sr_3Sc_2O_5)Fe_2As_2$ are shown in the nonmagnetic (left) and stripe antiferromagnetic state (right), with the arrows denoting the directions of spin moments.

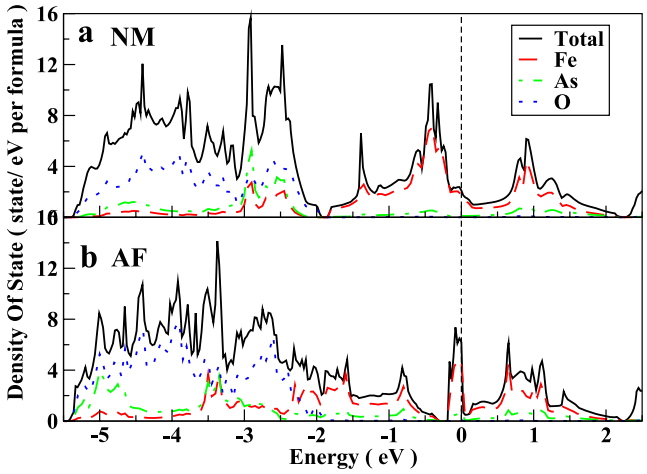

Figure 2. The total and projected density of state of $(Sr_3Sc_2O_5)Fe_2As_2$ in the NM state (a) and stripe AF state (b).

Table 1. The experimental and optimized atomic positions in the cell of tetragonal (space group $I4/mmm$, $Z = 2$) layered nonmagnetic phase.

Atom	Site	x	y	z (Exp.)	z (Opti.)
Sc	4e	0	0	0.073 99	0.074 74
Fe	4d	0.5	0	0.25	0.25
Sr	2b	0.5	0.5	0	0
Sr	4e	0.5	0.5	0.140 06	0.142 80
As	4e	0	0	0.200 18	0.205 88
O	8g	0.5	0	0.083 23	0.085 52
O	2a	0	0	0	0

LaFeAsOF ($T_C = 26$ K). Fortunately $(Sr_3Sc_2O_5)Fe_2As_2$ has been fabricated and its temperature dependence of resistivity, magnetization, Hall effect and magnetoresistance has also been measured [15]. Although superconductivity has not been discovered in $(Sr_3Sc_2O_5)Fe_2As_2$, it is expected to become a superconductor with electron or hole doping [15, 21].

It is well known that electronic structures are crucial to understand the physical properties of materials. The theoretical calculations that can provide further details about the electronic structure and related physical properties therefore are highly desirable. So far, no first-principles calculations for $(Sr_3Sc_2O_5)Fe_2As_2$ are reported on its stripe antiferromagnetic. In the present work, we employed the first-principles technique to investigate the band structure, Fermi surface and Lindhard response function of this compound. The Fermi surfaces are similar to those of LaFeOAs [22]: three hole-like Fermi surfaces around Γ-point and two electron-like Fermi surfaces around the X-point (corresponding to the M-point in LaFeOAs). The Fermi surface of $(Sr_3Sc_2O_5)Fe_2As_2$ shows very well the 2D character, while those of LaFeOAs appear dispersed along K_z. This difference may be because the spacing distance between FeAs layers is increased, which reduces the coupling between neighboring FeAs layers and increases the 2D character. The calculated Lindhard response function peaks at the X-point, which means a strong Fermi surface nesting effect and the possibility of competition between SDW and superconductivity [23]. When calculating the Lindhard response function we used the simplified formula without matrix elements, which had been proved as a useful method in the LaFeAsO system [23]. We calculated the electronic structure of the possible stripe antiferromagnetic (AF) state and found the energy of the AF state is 0.2075 eV (per Fe atom) favored than that of the NM state and the moment of the Fe atom is 2.2 μ_B. For LaFeAsO, the stabilization energy of the AF state is 0.180 eV in the experimental structure with the generalized gradient approximation GGA calculation. The stabilization energy of $(Sr_3Sc_2O_5)Fe_2As_2$ is larger than that of LaFeAsO, which may due to the moment of the Fe atom in the former (2.2 μ_B) being larger than in the latter (1.7 μ_B) [22]. The calculations are done with the BSTATE code, in the ultra-soft pseudopotential plane wave method [24] with experimental lattice constant and internal-atom positions [15]. The generalized gradient approximation for the exchange–correlation potential in the PBE form [25] is used. After carefully checking the convergence of calculated results with respect to the cutoff energy and the number of k-points, we adopt a cutoff energy of 30 Ryd for all the states and Monkhorst–Pack k-points generated with $8 \times 8 \times 12$ and $8 \times 8 \times 4$ for the NM and AF state, respectively.

Figure 1 shows the crystal structures of $(Sr_3Sc_2O_5)Fe_2As_2$ in the nonmagnetic (figure 1(a)) and in the stripe antiferromagnetism (figure 1(b)) phase. By minimizing the total energy versus cell volume with GGA of PBE type for the exchange–correlation potential we get the optimized lattice parameters ($a = 4.0820$ Å, $c = 26.7370$ Å) and internal coordinates (presented in table 1), which reasonably agree with the experimental results [15]. In figure 1, Fe atoms lie on a square sublattice coordinated tetrahedrally by As atoms, which is similar to that of $LnFeAsO_{1-x}F_x$ and $A_{1-x}K_xFe_2As_2$. The significant difference is that the FeAs layers are stacked with $Sr_3Sc_2O_5$ blocks along the c axis, which increases d_{FeAs} to as large as 13.438 Å. As mentioned above, the larger d_{FeAs} may induce a higher T_C.

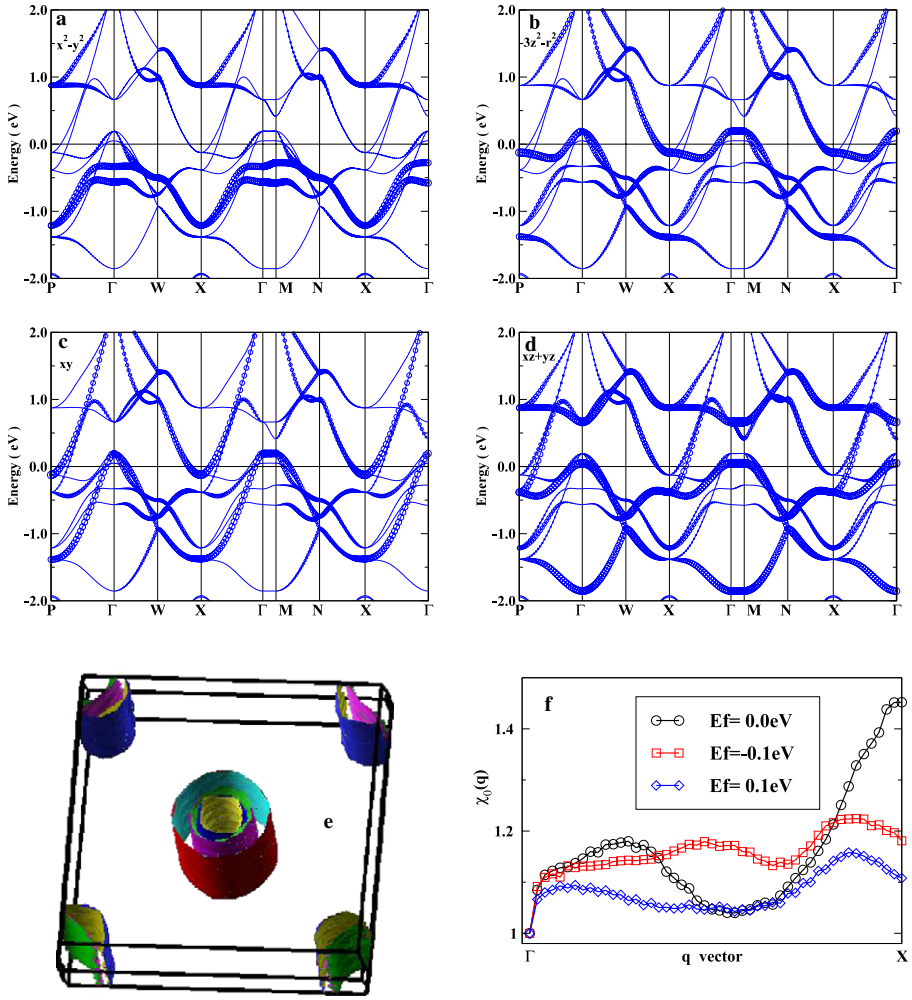

Figure 3. The projected bands, where the symbol size corresponds to the projected weight of Bloch states onto the $d_{x^2-y^2}$ (a), $d_{3z^2-r^2}$ (b), d_{xy} (c) and d_{yz+zx} (d). (e) The Fermi surface of the NM state. (f) The calculated Lindhard response function along the Γ–X line. The orientation of the coordinate system is chosen so that the Fe–Fe bonds are directed along the x and y axes.

To understand the electronic structures, we show the total and projected density of states (PDOS) of the NM state in figure 2(a). Both the total DOS and PDOS of $(Sr_3Sc_2O_5)Fe_2As_2$ are similar to those of $LnFeAsO_{1-x}F_x$ and $A_{1-x}K_xFe_2As_2$. Let us first focus on the states between −2 and +2 eV because the property of the compound is determined by the DOS near the Fermi level. It is obvious that this part of the DOS is mostly derived from Fe 3d states, just below which (from −6 to −2 eV) are the states of O p and As p. The p–d hybridization between O and Fe is negligible, while that between As and Fe is sizable. The calculated DOS at the Fermi level is $N(E_f) = 2.11\ \text{eV}^{-1}$ per formula unit of both spins. The corresponding bare susceptibility and specific heat coefficient are $\chi_0 = 6.8 \times 10^{-5}$ emu mol^{-1} and $\gamma_0 = 5.2$ mJ K^{-2} mol^{-1}, while in LaFeAsO [22] $\chi_0 = 8.5 \times 10^{-5}$ emu mol^{-1} and $\gamma_0 = 6.5$ mJ K^{-2} mol^{-1}. Because the Fermi level locates at the slope, hole doping will increase the DOS at the Fermi level $N(E_f)$, and in contrast electron doping will decrease $N(E_f)$. In $LnFeAsO_{1-x}F_x$ and $A_{1-x}K_xFe_2As_2$ the ground states of undoped compounds are stripe AF. Similarly, the calculated total energy of the stripe AF is 0.2075 eV (per Fe) lower than that of the NM solution. In figure 2(b), a pseudo-gap is opened just above E_f, which results in the AF solution being more stable. In the DOS of the AF state, while just below E_f, there is a sharp peak, which is mostly derived from the Fe 3d state. Compared with the NM solution, we find the p–d hybridization between As and Fe is reduced in the AF state, which makes the bands of Fe 3d more narrow in the AF state than in that of the NM solution.

The projected bands, Fermi surface and Lindhard response function are shown in figure 3. The derived bands do not split simply into lower e_g ($d_{x^2-y^2}$ and $d_{3z^2-r^2}$) and higher t_{2g} manifolds, as predicted by crystal field theory. Because of the presence of Fe–Fe bounds, the $d_{x^2-y^2}$ orbitals create bonding–antibonding bands located at −1 and +1 eV and these bands do not cut across the Fermi level. The Fermi surfaces are mostly derived not only from d_{xy} and d_{yz+zx} but also from $d_{3z^2-r^2}$. However, in LaFeAsO the Fermi surfaces mostly come from only d_{xy} and d_{yz+zx} orbitals [26, 27]. So, if $(Sr_3Sc_2O_5)Fe_2As_2$ becomes a superconductor, its pair mechanism may be different from that of LaFeAsO [30]. Such a difference may be due to the tetrahedral configuration being a little elongated than in LaFeAsO, because the distances between the As atom and the Fe layer are 1.32 Å and 1.34 Å

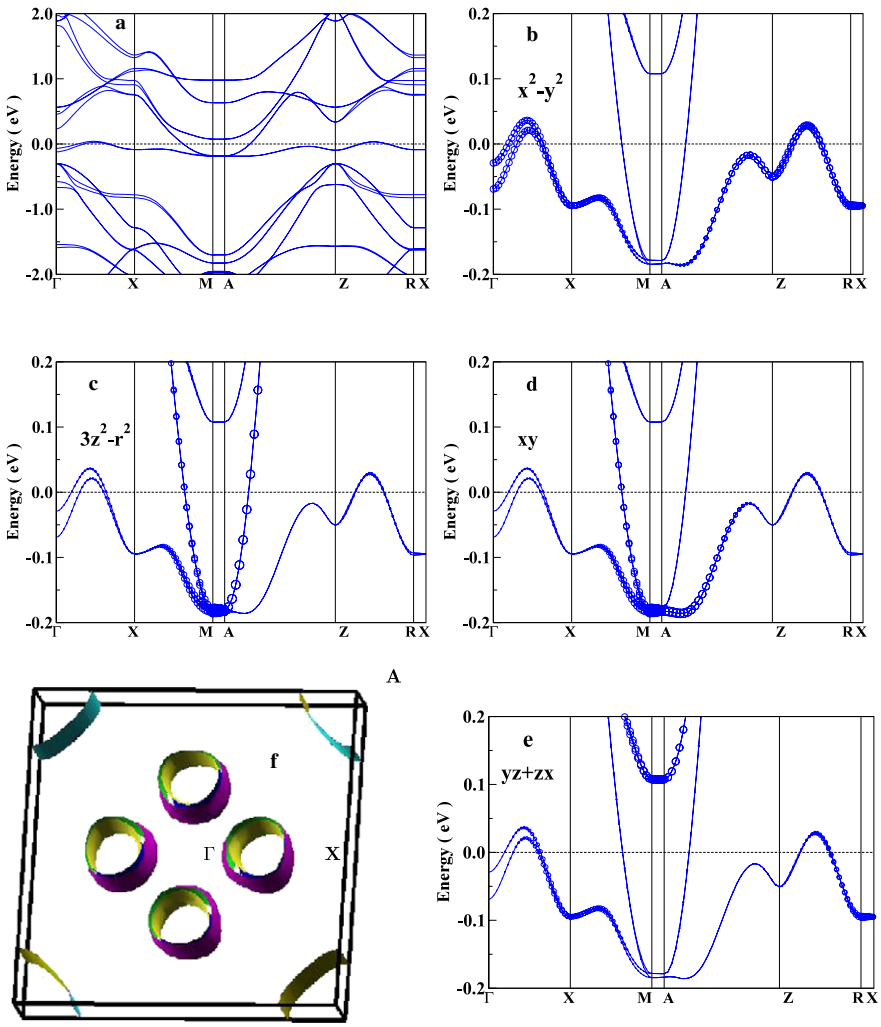

Figure 4. The band structure of the AF state along high symmetry directions (a). We plot the projected bands, where the symbol size corresponds to the projected weight of Bloch states onto the $d_{x^2-y^2}$ (b), $d_{3z^2-r^2}$ (c), d_{xy} (d) and d_{yz+zx} (e). The Fermi surface of the AF state (f). The orientation of the coordinate system is chosen so that the Fe–Fe bonds are directed along the x and y axes.

for LaFeAsO and $(Sr_3Sc_2O_5)Fe_2As_2$, respectively. The Fermi surfaces of $(Sr_3Sc_2O_5)Fe_2As_2$ in figure 3(e) are similar to those of LaFeAsO [22, 28], where three hole-like Fermi surfaces circle around Γ and two electron-like Fermi surfaces circle around X. By shifting the Fermi surfaces around Γ to X, i.e. by a vector $q = (\pi, \pi, 0)$, the hole-like Fermi surfaces will largely overlap with the electron-like Fermi surfaces, suggesting a significant nesting effect. Such a nesting effect can be quantitatively estimated by calculating the Lindhard response function $\chi_0(q)$ as shown in figure 3(f), where $\chi_0(q)$ is strongly peaked at the X-point for undoped compound, and it is obviously suppressed and becomes slightly incommensurate for both electron doping and hole doping. The author [15] did not find an SDW state maybe because there are some impurities or oxygen deficiencies in their sample (they also mentioned this possibility in their following work [20]). The suppression of $\chi_0(q)$ with electron doping can be understood with 'rigid' band shifting, because electron doping shifts the Fermi level up, which tends to reduce the size of hole-like Fermi surfaces and enlarge electron-like Fermi surfaces, and it reverses with hole doping. The existence of a strong nesting effect would suggest that certain kinds of ordering, such as charge density wave (CDW) or SDW [22, 23], may develop at low temperature in the undoped compound, just like LaFeAsO [22, 23, 29]. So we will study the electronic structure of $(Sr_3Se_2O_5)Fe_2As_2$ in the stripe AF ordering in the next paragraph.

The density of state of the AF state has been comparatively studied with that of the NM state in figure 2(b). Now we focus on the band structure and Fermi surfaces of the AF state, as shown in figure 4. The Fermi surface of the AF state is shown in figure 4(f), where two hole-like Fermi surfaces are located between the Γ-and X-points and two electron-like Fermi surfaces circle along the M–A line. Since the Fe atoms are coordinated by an As tetrahedron, the crystal field will normally split the five d-orbitals into low-lying twofold e_g states and up-lying threefold t_{2g}. However, the As tetrahedron is actually distorted from its normal shape (squeezed along c). This distortion will further split the e_g and t_{2g} manifolds significantly, making the final orbital distributions complicated. There are four bands crossing the Fermi level, with two 'narrow' bands and two 'expanding' bands. In order to study which orbitals play important roles

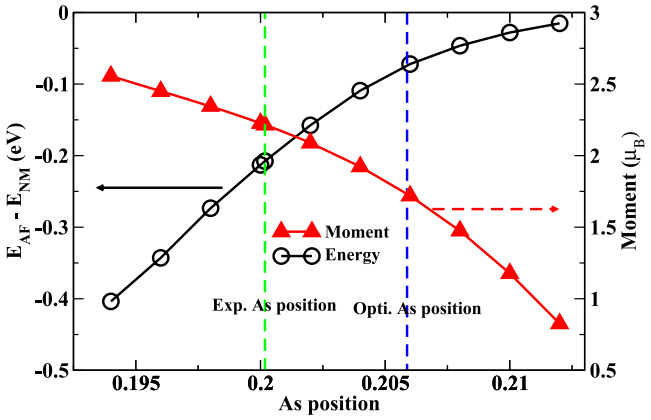

Figure 5. The stabilization energy (per Fe atom) and the moment of Fe atom changed with As coordinates.

in the 'narrow' bands and in the 'expanding' bands, we plot the projected bands, where the symbol size corresponds to the projected weight of Bloch states onto $d_{x^2-y^2}$, $d_{3z^2-r^2}$, d_{xy} and d_{yz+zx}. In the AF state, the orbital character shows significant difference with that of the NM state, where the Fermi surfaces between the Γ-point and X-point are mostly derived from the $d_{x^2-y^2}$ orbital and the Fermi surfaces along the M–A line mostly come from $d_{3z^2-r^2}$.

As discussed by Mazin *et al* [26], the internal coordination of As is important to determine the electron structure of the Fe-base superconductor. So we studied how the stabilization energy and the moment of the Fe atom changed with As coordinates with the lattice constant and coordinates of the other atoms fixed to their experimental values. In figure 5, we can see both the stabilization energy and the moment of the Fe atom decrease with the As atom moving to the Fe atom sheet. At the experimental position, the stabilization energy and the moment are 0.2075 eV and 2.2 μ_B, respectively. However, when the As atom shifts to the theoretically optimized position the stabilization energy and the moment are reduced to 0.072 eV and 1.72 μ_B, respectively.

In summary, by the first-principles calculations, we have studied the electronic structure of $(Sr_3Sc_2O_5)Fe_2As_2$, and found that its Fermi surfaces are very similar to those of LaFeAsO, while the projected bands show some differences. The Fermi surface nesting and the calculated $\chi_0(q)$ indicate SDW may exist in this undoped compound. The SDW will be suppressed greatly with either hole doping or electron doping. The previous authors did not find the SDW state, maybe because there are some impurities or oxygen deficiencies in their sample. By projecting the weight of Bloch states onto $d_{x^2-y^2}$, $d_{3z^2-r^2}$, d_{xy} and d_{yz+zx} orbitals, we find the $d_{x^2-y^2}$ orbital plays an important role in the two hole-like Fermi surfaces ('narrow' bands), while the $d_{3z^2-r^2}$ orbital mostly contributes to the two electron-like Fermi surfaces ('expanding' bands). Similar to LaFeAsO, both the stabilization energy and the moment of the Fe atom are very sensitive to the As atom position. Because of so much similarity to LaFeAsO, $(Sr_3Sc_2O_5)Fe_2As_2$ is expected to become a possible parent phase of a new type of FeAs-based superconductor.

Acknowledgment

The authors acknowledge the support from the NSF of China (no. 10674042).

References

[1] Kamihara Y, Watanabe T, Hirano M and Hosono H 2008 *J. Am. Chem. Soc.* **130** 3296
[2] Chen X H, Wu T, Wu G, Liu R H, Chen H and Fang D F 2008 *Nature* **453** 761
[3] Chen G F, Li Z, Wu D, Li G, Hu W Z, Dong J, Zheng P, Luo J L and Wang N L 2008 *Phys. Rev. Lett.* **100** 247002
[4] Ren Z A *et al* 2008 *Europhys. Lett.* **82** 57002
[5] Ren Z A *et al* 2008 *Chin. Phys. Lett.* **25** 2215
[6] Rotter M, Tegel M, Johrendt D, Schellenberg I, Hermes W and Pöttgen R 2008 *Phys. Rev.* B **78** 020503(R)
[7] Rotter M, Tegel M and Johrendt D 2008 *Phys. Rev. Lett.* **101** 107006
[8] Sasmal K, Lv B, Lorenz B, Guloy A M, Chen F, Xue Y Y and Chu C W 2008 *Phys. Rev. Lett.* **101** 107007
[9] Ding H *et al* 2008 *Europhys. Lett.* **83** 47001
[10] Xu G, Zhang H J, Dai X and Fang Z 2008 *Europhys. Lett.* **84** 67015
[11] Wu G, Liu R H, Chen H, Yan Y J, Wu T, Xie Y L, Ying J J, Wang X F, Fang D F and Chen X H 2008 *Europhys. Lett.* **84** 27010
[12] Tapp J H, Tang Z J, Lv B, Sasmal K, Lorenz B, Chu P C W and Guloy A M 2008 *Phys. Rev.* B **78** 060505(R)
[13] Wang X C, Liu Q Q, Lv Y X, Gao W B, Yang L X, Yu R C, Li F Y and Jin C Q 2008 *Solid State Commun.* **148** 538
[14] Hsu F C *et al* 2008 *Proc. Natl Acad. Sci. USA* **105** 14262
[15] Zhu X, Han F, Mu G, Zeng B, Cheng P, Shen B and Wen H H 2009 *Phys. Rev.* B **79** 024516
[16] Ogino H, Matsumura Y, Katsura Y, Ushiyama K, Horii S, Kishio K and Shimoyama J 2009 arXiv:0903.3144
[17] Ogino H, Katsura Y, Horii S, Kishio K and Shimoyama J 2009 arXiv:0903.5124
[18] Chen G F, Xia T L, Zheng P, Luo J L and Wang N L 2009 arXiv:0903.5273
[19] Xie Y L *et al* 2009 arXiv:0903.5484
[20] Zhu X Y, Han F, Mu G, Cheng P, Shen B, Zeng B and Wen H H 2009 arXiv:0904.1732
[21] Shein I R *et al* 2009 arXiv:0903.4038
Shein I R *et al* 2009 arXiv:0903.4475
Shein I R *et al* 2009 arXiv:0904.0117
Shein I R *et al* 2009 arXiv:0904.2671
[22] Singh D J and Du M H 2008 *Phys. Rev. Lett.* **100** 237003
Xu G *et al* 2008 *Europhys. Lett.* **82** 67002
[23] Dong J *et al* 2008 *Europhys. Lett.* **83** 27006
de la Cruz C *et al* 2008 *Nature* **453** 899
[24] Fang Z and Terakura K 2002 *J. Phys.: Condens. Matter* **14** 3001
[25] Perdew J P, Burke K and Ernzerhof M 1996 *Phys. Rev. Lett.* **77** 3865
[26] Mazin I I, Johannes M D, Boeri L, Koepernik K and Singh D J 2008 *Phys. Rev.* B **78** 085104
[27] Boeri L, Dolgov O V and Golubov A A 2008 *Phys. Rev. Lett.* **101** 026403
Vildosola V, Pourovskii L, Arita R, Biermann S and Geroges A 2008 *Phys. Rev.* B **78** 064518
[28] Dai X, Fang Z, Zhou Y and Zhang F C 2008 *Phys. Rev. Lett.* **101** 057008
[29] Ma F and Lu Z Y 2008 *Phys. Rev.* B **78** 033111
[30] Kuroki K, Onari S, Arita R, Usui H, Tanaka Y, Kontani H and Aoki H 2008 *Phys. Rev. Lett.* **101** 087004
Daghofer M, Moreo A, Riera J A, Arrigoni E, Scalapino D J and Dagotto E 2008 *Phys. Rev. Lett.* **101** 237004
Wang F, Zhai H, Ran Y, Vishwanath A and Lee D H 2009 *Phys. Rev. Lett.* **102** 047005
Boyd G R, Devereaux T P, Hirschfeld P J, Mishra V and Scalapino D J 2009 *Phys. Rev.* B **79** 174521